Craze fibril breakdown in glassy polymers

C. J. G. Plummer and A. M. Donald*
University of Cambridge, Cavendish Laboratory, Madingley Road, Cambridge CB3 0HE, UK
(Received 21 December 1989; accepted 15 August 1990)

Recent work suggests that the origin of fibril breakdown is disentanglement of polymer chains in the 'active zone' at the craze–bulk interface, where the deformation ratio of the polymer is increasing towards that of the fully formed fibril, and the polymer is in a strain-softened state (that is, the chains are relatively mobile). Since disentanglement times are expected to be strongly dependent both on temperature and on the molecular weight of the chains in the fibril, it is clear that these parameters should also strongly affect fibril stability. We have investigated craze fibril breakdown as a function of molecular weight and temperature in thin films of polystyrene and poly(ether sulphone), and have found good qualitative agreement between our results and a molecular model for fibril breakdown based on the earlier ideas of Kramer and Berger.

(Keywords: crazing: craze stability; entanglement; reptation; polystyrene; poly(ether sulphone)

INTRODUCTION

It is well known that a qualitative link exists between the onset of embrittlement in amorphous glassy polymers and crazing. The open voided structure of crazes makes them potential nucleation sites for cracks and hence, when a sample is placed under tensile stress, the appearance of crazes often leads to unstable crack growth and fracture. However, the crazes themselves are often capable of bearing significant loads, so that any criterion for brittle behaviour must take into account not only the critical stress for crazing but also the kinetics of the craze fibril breakdown, which must necessarily precede crack nucleation. In what follows, we describe an investigation into craze fibril stability in thin films of polystyrene (PS) and poly(ether sulphone) (PES) for a range of temperatures and molecular weights, and discuss the results in terms of a reptation model for fibril breakdown.

CRAZING AND ENTANGLEMENT LOSS

Underpinning many current ideas regarding phenomena associated with both craze growth and craze stability is the concept of entanglement, which refers to the topological constraint on relative chain motion. Because a craze is an open voided structure, crazing is generally associated with a certain degree of 'geometrically necessary entanglement loss'[1]. This is of crucial importance for craze stability since the load-bearing capacity of craze fibrils is dependent on the extent to which forces can be transmitted between individual chains via entanglement[1].

Kramer and coworkers[1–4] first demonstrated the importance of entanglement loss in their work on ambient-temperature crazes in low-entanglement-density polymers such as PS. These observations were rationalized in terms of a surface drawing mechanism for craze widening[1], illustrated in *Figure 1*, craze widening generally being accepted to control the rate of craze propagation into the bulk polymer[5,6]. Polymer in a thin strain-softened layer at the craze–bulk interface is assumed to flow along the gradient in hydrostatic tension between the fibril bases and the interfibrillar void tips, and, as the polymer moves away from the void tips and into the fibrils, the craze widens. On this basis Kramer has shown that the critical stress for craze propagation S_c obeys[1]:

$$S_c = f(T, \dot{\varepsilon})\Gamma^{1/2} \quad (1)$$

where Γ is the effective surface energy at the void tip, and $f(T, \dot{\varepsilon})$ is a front factor weakly dependent on temperature T and strain rate $\dot{\varepsilon}$.

Now consider the two chains A and B shown schematically in *Figure 1*. These are assumed to be subject to a constraint on their relative motion represented by the 'entanglement point' at C. This view presupposes the entanglement network model in which topological constraints on relative chain motion are treated as analogous to chemical crosslinks. Thus the polymer is viewed as a network of strands linked at entanglement points. Implicit in this network approach is the immutability of the entanglements, so that in order for the craze to continue to widen in *Figure 1*, chain scission must take place. More generally, all such entangled strands crossing the surface of the primordial cylinder, of diameter D_0 shown in *Figure 1*, are expected to undergo scission. Hence the force per entangled strand in the surface at the void tip will be approximately equal to the force for chain scission, which leads to the following expression for the surface energy at the void tip[1]:

$$\Gamma = \Gamma_0 + U d_e v_e / 4 \quad (2)$$

where Γ_0 is the van der Waals surface energy, U is the bond energy, d_e is the entanglement separation and v_e is the entanglement density. Then Γ may be substituted in equation (1) to obtain the crazing stress.

While equation (2) has been used successfully to describe room-temperature crazing in PS, more recently, disentanglement by reptation has been shown to play an important role in entanglement loss during crazing in low-molecular-weight glassy polymers close to T_g[7–13]. Here 'reptation' is used as a generic term to refer to any mechanism of disentanglement in which a given chain

* To whom correspondence should be addressed

0032-3861/91/030563-10

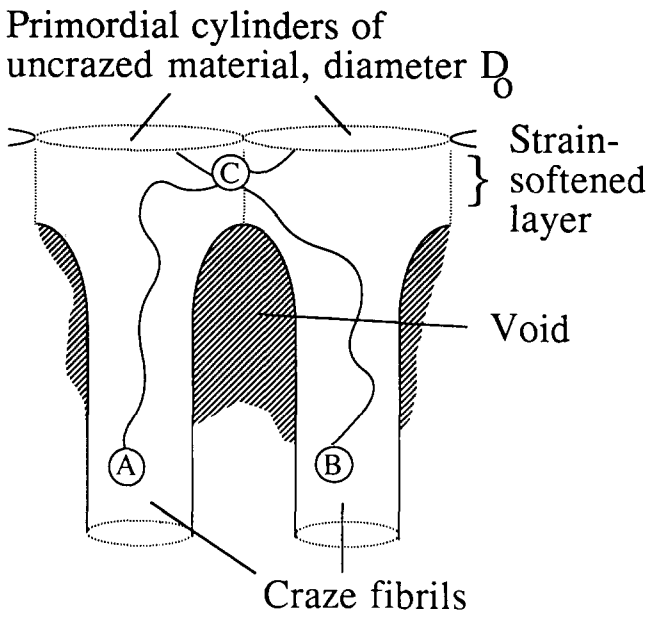

Figure 1 A schematic representation of the surface drawing mechanism during craze widening. Polymer in the thin strain-softened layer at the craze–bulk interface flows toward the fibril bases along the gradient in hydrostatic tension between the void tips and the fibril bases. The chains marked A and B and entangled at C must either break or disentangle in order to continue to move into adjacent fibrils as shown

may be visualized as moving along the length of a virtual confining tube representing the topological constraint on that chain arising from its interactions with neighbouring chains[14,15]. To describe entanglement loss during crazing, McLeish *et al.* introduced the idea of 'forced reptation'[16]. They assumed that one end of a disentangling chain was anchored by work hardening in the filament, and that the remainder of the chain was pulled out of its confining tube at a rate v as the craze–bulk interface advanced. They then argued that the force f_d acting along the chain is given by[16]:

$$f_d \sim v\zeta_0 M/M_0 \tag{3}$$

where ζ_0 is a monomeric friction coefficient, M_0 is the monomer molecular weight and M is the molecular weight of the chain. For chain scission, the force to break a bond is approximately:

$$f_b \sim U/(2a) \tag{4}$$

where a is the bond length[7]. If $f_d < f_b$, disentanglement will take place in preference to scission. Assuming the velocity v of the chain relative to its tube to be proportional to the applied deformation rate $\dot{\varepsilon}$, one can see immediately from equations (3) and (4) that disentanglement will be favoured by low $\dot{\varepsilon}$, low M and high temperature T, through the term ζ_0, which may be written as $A\exp(E/RT)$, where E is a characteristic activation energy[16]. This approach was developed by Kramer and Berger[7], who showed that equation (2) remains valid at low T, but that as T is raised there is a transition to disentanglement mediated crazing, characterized by a sharp drop in Γ, and this transition is strongly dependent on M and $\dot{\varepsilon}$. Eventually, as T is raised further, a regime where $\Gamma \sim \Gamma_0$ is predicted, the so-called 'van der Waals' regime[7,8,16].

Whilst the model of Kramer and Berger is in good qualitative accord with observations of the crazing behaviour as a function of T, M and $\dot{\varepsilon}$, and the competition between crazing and shear deformation in a variety of polymers[7–13], and also predicts the right magnitude for the drop in Γ as the scission to disentanglement transition is crossed[7], it is based on the unrealistic assumption that any given chain will only cross the surface of the primordial cylinder in *Figure 1* once. Numerical calculations, based on the network model and the assumption that the strands linking entanglement points are Gaussian random walks, suggest that approximately half of all entangled strands in PS cross the surface of the primordial cylinder[17,18]. For molecular weights of PS typical, for example, of the experimental observations of Kramer and Berger[7], M is greater than $5M_e$, where M_e is the molecular weight of the network strands. Therefore, on average, a given chain in such a material will cross the surface of the primordial cylinder more than 2.5 times. For the high-entanglement-density polymer PES, an average of approximately 10 crossings per chain is expected (for the molecular weights available there are approximately 30 entanglement points per chain).

The effect of multiple crossing is modelled as illustrated in two dimensions in *Figure 2*. The entanglement constraint is represented as a regular distribution of points that the chain is unable to cross, which deform affinely as the craze–bulk interface advances, moving apart at an average velocity v. The multiple chain crossing of the plane of separation, which represents the surface of the primordial cylinder in *Figure 2*, results in the amplification of the chain contour velocity along the length of the chain via a 'block-and-tackle' mechanism[7,16], and in the limit of a large number of crossings of the plane of separation by each chain, one can show

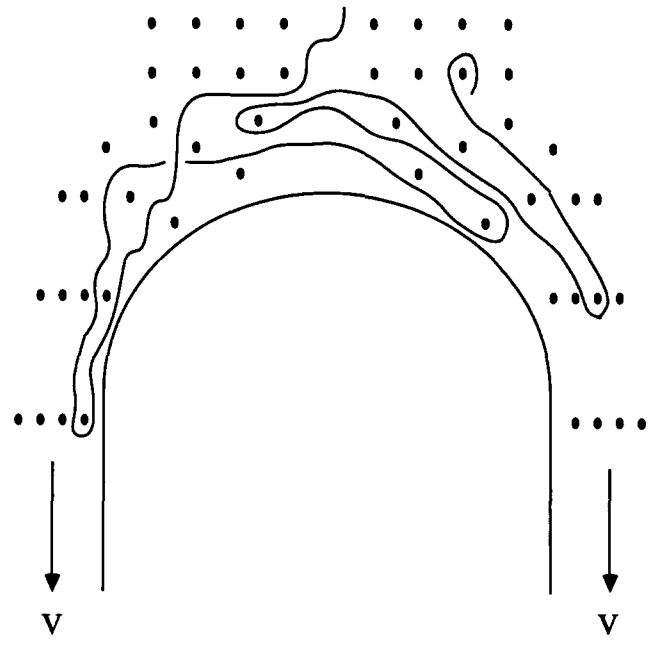

Figure 2 The effect of multiple crossing on the disentanglement mechanism. The effect of entanglement is represented by an array of point constraints that the chain is not allowed to cross, which deform affinely with the strain-softened layer as the craze–bulk interface advances. As the void advances, successive loops of the chain shown will be pulled in opposite directions as we move along the length of the chain. Thus we may approximate the behaviour of the chain by the 'block-and-tackle' mechanism

that this leads approximately to:

$$\langle f \rangle \sim \zeta_0 v M^2 / 24 M_0 M_c \quad (5)$$

and

$$f_{max} \sim \zeta_0 v M^2 / 16 M_0 M_c \quad (6)$$

where $\langle f \rangle$ is the mean force in the chain, f_{max} is the maximum force in the chain (that is, the force at the mid-point of the chain) and M_c is the mean molecular weight between crossing points[7]. Thus the disentanglement contribution to Γ is expected to scale as approximately M^2 rather than as M, as suggested by equation (3).

In order to take into account chain scission, it is assumed that chain scission will occur randomly until f_{max} in the resulting chain fragments becomes of the order of or less than the force for scission (equation (4)). It is convenient therefore to define a critical molecular weight M_{crit} such that:

$$\frac{U}{2a} = f_{max}(M_{crit}) = \frac{\zeta_0 v M_{crit}^2}{16 M_c M_0} \quad (7)$$

and it is assumed that, for $M > M_{crit}$, the number of scissions per chain will be of the order of M/M_{crit}. Since the number of times a given chain will intersect the plane of separation is M/M_c, the proportion of strands crossing the plane of separation undergoing scission is estimated to be M_c/M_{crit} so that:

$$\Gamma = \Gamma_0 + \frac{d_e v_e U}{4} \frac{M_c}{M_{crit}} + \Gamma_d \quad (8)$$

where Γ_d represents additional contributions to Γ from disentanglement of the chain fragments[19], and will tend to zero as M_{crit} tends to M_c with decreasing T (that is, when all the strands crossing the plane of separation undergo chain scission), so that in this limit, equation (8) gives equation (2). As T increases on the other hand, and M_{crit} becomes greater than M, no scission will occur and Γ_d can be calculated directly from equation (5)[19]. Since Γ_d is decreasing exponentially with T there will be a high-temperature 'van der Waals' regime where $\Gamma \sim \Gamma_0$.

Essentially then, this model predicts similar qualitative behaviour to Kramer and Berger's model. However, by taking account of multiple crossings we obtain a more realistic model for the molecular-weight degradation in regimes of mixed disentanglement and scission. As will be seen in the next section, this is of considerable importance for modelling craze stability.

CRAZE FIBRIL BREAKDOWN

We now consider the statistics and molecular mechanisms of fibril breakdown, as deduced by Kramer and coworkers from previous experimental observations of fibril breakdown in thin films of polymer mounted on copper grids (the technique will be described in more detail in the 'Experimental' section). In such experiments, the criterion for breakdown in a given grid square is the appearance of at least one breakdown event within the crazes formed in that square.

The statistics of craze fibril breakdown

Clearly it is reasonable to assume that individual fibrils are statistically independent of each other, and also that regions along the length of a given fibril separated by more than the 'entanglement transfer length' (of the order of the entanglement separation d_e) are statistically independent[1,7,20]. The total number of statistically independent potential sites for fibril breakdown will therefore increase as ε_p, the plastic strain in the film resulting from crazing, given by $\varepsilon - \varepsilon_c$ (where ε_c is the strain at which the crazes appear). Kramer and others have also assumed that the stress in the film will increase with ε_p according to a power law[7,20]:

$$S = S_1 \varepsilon_p^w \quad (9)$$

where S_1 is the stress when $\varepsilon_p = 1$, and w is of the order of 0.1. They then postulated that p_b, the probability of breakdown of a given entanglement transfer length, should also show some power-law dependence on ε_p:

$$p_b(S) = p_b(S_1) \varepsilon_p^{\rho_w - 1} \quad (10)$$

where the power-law exponent is written as $\rho_w - 1$ for convenience. The probability of one or more fibril breakdown events in a grid square, $P_b(\varepsilon_p)$, can be argued on this basis to be governed by a Weibull distribution[21], such that the median value of ε_p for breakdown, which is termed ε_{pb}, is given by[7]:

$$\varepsilon_{pb} = \left(\frac{(\lambda - 1)\rho_w \ln 2}{n_f V_0 p_b(S_1)} \right)^{1/\rho_w} \quad (11)$$

where V_0 is the volume of a grid square at zero strain, λ is the fibril extension ratio, n_f is the number of entanglement transfer lengths per unit volume of crazed material and ρ_w in equation (10) becomes the Weibull modulus, which can be determined by plotting $\ln \varepsilon_p$ against experimental data for $\ln\{\ln[1 - P_b(\varepsilon_p)]^{-1}\}$. It has been shown to be approximately 5 in PS at room temperature[7,20].

Molecular mechanisms of breakdown in scission crazes

In the limit of entanglement loss being mediated entirely by scission, it is simple to show [1] that:

$$\frac{1}{M_n(i)} = \frac{1}{M_n} + \frac{1 - iq/n_e}{M_e} \quad (12)$$

where M_n is the number-average molecular weight prior to fibrillation, M_e is the molecular weight between entanglements, q is the probability that a given entangled strand survives scission during fibrillation, n_e is the mean number of entangled polymer strands crossing a fibril cross-section and i is the number of such strands locally that remain entangled subsequent to fibrillation[1].

In any given fibril, i will vary along the length of a given fibril, giving rise to weak spots where relatively few strands are entangled, and hence able to bear loads, in a given fibril cross-section[1,7,20]. Kramer and Berger argue that the following Gaussian form approximates the variation in i along any given fibril[7]:

$$\phi(i)\,\mathrm{d}i = \frac{1}{[2\pi(1-q)n_e]^{1/2}} \exp\left(\frac{-(i - n_e)^2}{2(1-q)n_e} \right) \mathrm{d}i \quad (13)$$

For PS, q is taken to be 0.6 and n_e is given by $n_0 q(1 - M_e/qM_n)$, where n_0 is the total number of strands crossing the fibril cross-section, given by $\frac{1}{8}\pi D_0^2 v_e d_e$, and is approximately equal to 50 for typical room-temperature PS crazes[7].

Given that weak spots where i is relatively low exist in the fibrils, it is now necessary to consider the mechanism by which such weak spots may become

unstable and break down. The evidence of Kramer and coworkers suggests that breakdown occurs as a result of chain disentanglement in the 'stretch zone' at the craze–bulk interface[7,20], where the fibrillar material is being drawn towards its final extension ratio within the fibril. However, at a certain time t_{res} after a given chain has entered the stretch zone, where it will initially be in a strain-softened state and hence relatively mobile, it is argued that the chain becomes too immobile to undergo further disentanglement because of stress-ageing effects[7,20]. Thus if the disentanglement time for chains in the stretch zone is greater than t_{res} the fibril is assumed to remain stable.

For times less than t_{res} the chain will disentangle by the block-and-tackle mechanism. Chains in the stretch zone are again supposed to be subject to point constraints as shown schematically in *Figure 3*. Unlike the disentanglement occurring during fibrillation described above, however, the relative velocity of the point constraints on the chains will no longer be fixed by the craze widening rate. Instead, it is the total force acting on each fibril that will be fixed and equal to $\frac{1}{4}\pi D_0^2 S$ where S is the average stress in the film (given by equation (9)). This leads to:

$$\frac{1}{4i}\pi D_0^2 S = \frac{\zeta_0 v_f M(i)^2}{24 M_0 M_e} \tag{14}$$

where v_f is the relative velocity of the constraints in the fibril, $M(i)$ is given by equation (9) and M_e is the entanglement molecular weight, assumed here to be the effective molecular weight between the point constraints[7]. Clearly, as disentanglement proceeds, and as the point constraints move apart, M_e will increase, and eventually, when M_e becomes of the order of M, disentanglement will be complete, and the chain will no longer be load-bearing. The rate of change of M_e will be $dM_e/dt = v_f M_0/l_0$ where l_0 is the monomer length, so equation (14) can be written as:

$$\frac{1}{4i}\pi D_0^2 S M_e = \frac{\zeta_0 M(i)^2 l_0}{24 M_0^2}\frac{dM_e}{dt} \tag{15}$$

This has the solution:

$$M_e = M_e(0)\exp(t/\tau_{dis})$$

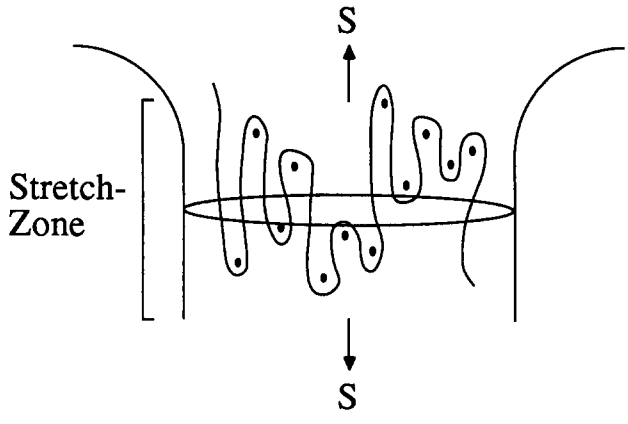

Figure 3 Schematic of the stretch zone in which chains have undergone 'geometrically necessary' entanglement loss by either scission or disentanglement, but are still able to disentangle at a finite rate by the block-and-tackle mechanism under the influence of the craze surface stress S_c. The shaded area represents the fibril cross-section

where

$$\tau_{dis}(i) = \frac{i\zeta_0 M(i)^2 l_0}{6 M_0^2 S\pi D_0^2}$$

which gives a crude time constant for disentanglement of these chains. In Kramer and Berger's more complete treatment[7] the disentanglement time is given by:

$$\tau_{dis}(i) = \frac{i\zeta_0 M(i)^2 l_0}{6 M_0^2 S\pi D_0^2}\left[3 + \ln\left(1 + \frac{M}{2M_e}\right)\right] \tag{16}$$

If $\tau_{dis}(i) < t_{res}$ the chains are assumed to be able to disentangle completely before work hardening sets in, and the fibril is hence assumed to fail if this criterion is met. Kramer and Berger express this by writing the probability of fibril failure for a given value of i as[7]:

$$p_b(i) = \exp[-\tau_{dis}(i)/t_{res}] \tag{17}$$

The value of p_b for a randomly chosen fibril can then be obtained by combining equations (13) and (17) and using:

$$p_b = \int_0^{n_0} \phi(i) p_b(i)\, di \tag{18}$$

Kramer and Berger have used equation (18) to calculate values of $p_b(S_1)$, taking S_1 to be approximately the craze initiation stress, and have combined these with the Weibull approach (equation (11)) to model the median strain for craze breakdown ε_{pb} for various molecular weights of PS at room temperature, treating t_{res} as an adjustable parameter[7]. They were able to obtain good fits to the observed increase of ε_{pb} in PS, poly(methyl methacrylate) (PMMA) and poly(α-methylstyrene) (PαMS) with M for $\dot{\varepsilon} = 3 \times 10^{-6}\ s^{-1}$, taking t_{res} to be 195, 88 and 364 s respectively[7]. This increase in craze stability with M had been reported previously[1,20,22,23] and for scission crazing is a direct consequence of the dependence of the fibrillar molecular weight on M via equation (9) and the assumption that breakdown is mediated by disentanglement.

Craze breakdown as a function of temperature

Two main effects need to be taken into account when considering the effect of temperature on craze stability. First, it is necessary to take into account that τ_{dis} increases as ζ_0, which will in turn be decreasing exponentially with T, so that, for a given fibrillar molecular weight, a strong decrease in fibril stability with T is expected. Secondly, it is necessary to take into account that as T is raised the degree of chain scission, and consequently the degree of molecular-weight degradation, will decrease as disentanglement becomes more favourable. This will tend to raise τ_{dis}, both because the mean value of the fibrillar molecular weight $M(i)$ will increase and also because the standard deviation of the distribution in $M(i)$ will decrease, so that there will tend to be fewer weak spots. Eventually, when scission has been entirely replaced by disentanglement, there should be no stochastic variation in the fibrillar molecular weight, and fibril breakdown will reflect the behaviour of the starting molecular weight rather than the extreme low $M(i)$ tail of a distribution.

This behaviour can be modelled in terms of the block-and-tackle mechanism for craze widening. At some arbitrary temperature then, the maximum molecular weight able to disentangle is (from equation (7)):

$$M_{crit} = (8UM_c M_0/\zeta_0 va)^{1/2} \tag{19}$$

and when $M_c < M_{crit} < M$ the total number of scissions is of the order of M/M_{crit}. Hence, in order to model the extent of molecular-weight degradation, M/M_{crit} is substituted for q in equations (12) and (13), when the above criterion is satisfied, and when $M < M_{crit}$, $\phi(i)$ is assumed to be a delta function at $i = n_0$ and $M(i)$ to be equal to M everywhere.

The quantities in equations (16) and (19) are now estimated for PS. Following Kramer and Berger[7], for PS, $E \sim 159$ kJ mol^{-1} and $A \sim 1.7 \times 10^{-28}$ N s m^{-1}, from which $\zeta_0 = A \exp(E/RT)$ may be obtained, and l_0 and M_0 are approximately 5×10^{-10} m and 104 respectively. At room temperature $S_1 \sim 40$ MPa and $D_0 \sim 20 \times 10^{-9}$ m for scission crazes formed in PS at a strain rate $\dot{\varepsilon} = 4.1 \times 10^{-6}$ s^{-1} (ref. 19). Because it is dominated by the strong T dependence of ζ_0, τ_{dis} is insensitive to the relatively weak variations in $S_1 D_0^2$ observed when T is raised[19,24], and so room-temperature values for S_1 and D_0 are used throughout.

The additional quantities required in equation (19) are $U \sim 6 \times 10^{-19}$ J for a carbon chain backbone[1], $M_c \sim 40\,000$, $a \sim l_0$ and $v \sim 10^{-9}$ m s^{-1} (for $\dot{\varepsilon} = 4 \times 10^{-6}$ s^{-1}). Hence the disentanglement time, τ_{dis}, is of the order of $8 \times 10^{-33} iM(i)^2 \exp(E/RT)$ at room temperature; the maximum molecular weight able to disentangle during fibrillation, M_{crit}, is of the order of $5 \times 10^{17} \exp(-E/2RT)$. This makes it possible to calculate $p_b(S_1)$ using equations (13), (17) and (18), and, again following Kramer and Berger, taking t_{res} as 2×10^2 s for PS[7]. Then ε_{pb} can be estimated from equation (11), taking ρ_w as 5[7,20] and λ as 4[1], and the remaining parameters from ref. 20.

The predicted dependence for ε_{pb} as a function of T for $M = 127\,000$ and $M = 1\,150\,000$ is plotted in *Figure 4*. At room temperature the values of ε_{pb} are relatively large, with ε_{pb} for $M = 1\,150\,000$ approximately three times greater than ε_{pb} for $M = 127\,000$. As the temperature is raised, ε_{pb} then decreases rapidly until $M \sim M_c$, at which point the curves flatten off (indeed there is even a slight increase in ε_{pb} in the temperature range 30 to 40°C). Finally, as M_c approaches M in each case, there is a very sharp peak in ε_{pb} beyond which ε_{pb} decreases rapidly, approaching zero close to T_g. For $M = 1\,150\,000$ this peak occurs above approximately 70°C, and for $M = 127\,000$ above approximately 40°C (the maximum predicted values of ε_{pb} are beyond the range of *Figure 4*, reaching values in excess of 10^3).

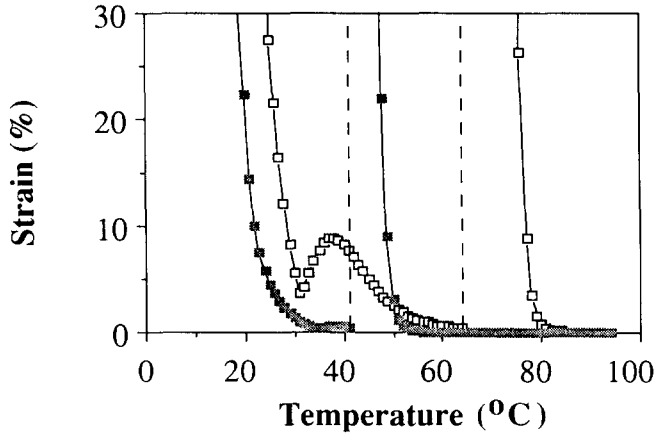

Figure 4 Calculated variation of the median strain for fibril breakdown ε_{pb} with temperature for PS of two different molecular weights, $M = 127\,000$ (■) and $M = 1\,150\,000$ (□)

To conclude this section, we summarize the model in physical terms. As T is raised close to room temperature, the effective molecular weight in the fibrils remains constant since the extent of scission is expected to be independent of T, and so the stability will decrease as the chain mobility increases. At higher T some disentanglement is possible and so the scission contribution to entanglement loss during fibrillation decreases. At the same time as the amount of scission decreases, the statistical scatter in the fibril molecular weight becomes smaller, so there is a tendency for the number of localized weak spots in the craze fibrils to diminish. Both effects offset the decrease in fibril stability with temperature expected from the increased mobility of the chains, and as the amount of scission tends to zero a sharp peak in stability is predicted. When the transition to disentanglement is complete, there can be no further changes in the fibrillar molecular weight or its distribution; the chain mobility is still increasing with T, however, and so the stability begins to decrease once more.

In general such peaks in stability are expected in any material showing a transition from scission to disentanglement crazing, and at temperatures corresponding to this transition, although in practice the peaks will be smoothed out somewhat, owing, for example, to statistical variations in the extent to which individual chains are involved in multiple crossing. In view of the many assumptions already implicit in the treatment, these additional variables are not considered quantitatively here.

EXPERIMENTAL

Craze stability has been examined as a function of T and M in PS (supplied by Polymer Laboratories Ltd) and PES (Victrex, supplied by ICI plc). In the case of PS, the samples were monodisperse with molecular weights of 127 000 and 1 150 000. Commercially available PES, on the other hand, being a condensation polymer, is highly polydisperse (with a polydispersity of the order of 2). Two differing molecular-weight distributions were used for these experiments, termed here M1 and M4 (to be consistent with the nomenclature of Davies and Moore[25]), for which the molecular-weight averages were 47 000 and 69 000 respectively. In order to increase this range somewhat, fractionation was carried out in the manner described by Davies and Moore[25], in order to separate the low-molecular-weight tail from M1, using dimethylformamide/ethanol as a solvent/non-solvent system for PES. For the weight fractions obtained, the molecular-weight average is estimated to be 25 000 from data for the molecular-weight distributions given by Davies and Moore[25].

Thin films, of the order of 0.4 μm in thickness, were made by letting a drop of a solution of the polymer in question fall onto a rotating glass slide (the speed of rotation of the slide controlled the film thickness). When the solvent had evaporated the resulting film was floated off on a water bath and picked up on a copper grid previously coated with the same polymer, to which the film was bonded, after drying, using a short exposure to the appropriate solvent vapour[26,27]. The solvents were toluene and cyclohexanone at 40°C for PS and PES respectively. When the films had been bonded to the

grids, they were placed in a vacuum oven for 12 h at $T_g - 20°C$ in order to dry them, and also to age them physically and hence to suppress shear deformation[8,28].

A spin-casting method was used since it is economical in terms of the amount of polymer required, and in particular since, by attaching a 0.2 μm filter to a syringe, it is possible to produce dust-free drops and hence dust-free films. That the films contain as few inhomogeneities as possible is important if one is to investigate the intrinsic fibril stability, rather than, for example, decohesion at dust particles[7,20]. The films, on their copper grids, were then strained at a constant strain rate of $4 \times 10^{-6}\ s^{-1}$, in an environmental chamber, while being observed using an optical microscope in both reflected and transmitted light. Subsequent to deformation and removal from the straining rig, the individual grid squares were examined using transmission electron microscopy (TEM).

RESULTS AND DISCUSSION

As in previous investigations of craze stability[7,20] the strain to craze ε_c and the number of grid squares in which fibril breakdown has occurred as a function of ε_p have been measured, from which ρ_w can be determined by plotting $\ln \varepsilon_p$ against data for $\ln\{\ln[1 - P_b(\varepsilon_p)]^{-1}\}$.

Results for polystyrene

Figures 5 and *6* show the strain to craze ε_c and the median strain for fibril breakdown ε_{pb} respectively. The data are for PS $M = 127\,000$ and $M = 1\,150\,000$ plotted against T. The following features are of particular note:

(i) As T increases from room temperature, both the high-M and the low-M data show an initial decrease in ε_{pb}, the decrease being more marked for $M = 1\,150\,000$, while ε_c remains approximately the same for both M.

(ii) At approximately 40°C there is a minimum in ε_{pb} for $M = 127\,000$ followed by a sharp maximum at approximately 45°C beyond which ε_{pb} decreases rapidly with T once more, becoming very close to ε_c as T approaches T_g. The minimum in ε_{pb} appears to correlate with the onset of a steep decrease in ε_c with T approximately 40°C.

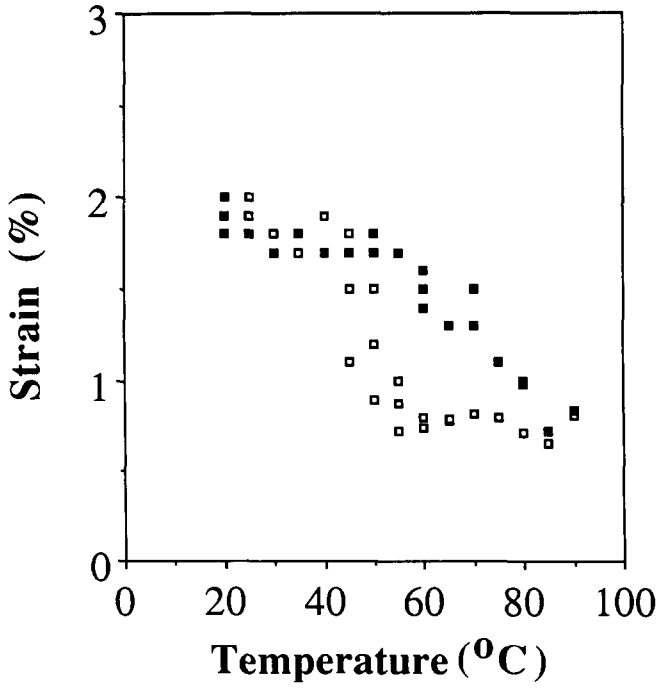

Figure 5 The strain to craze ε_c in PS as a function of temperature at a strain rate of $4 \times 10^{-6}\ m^2$ for $M = 127\,000$ (□) and $M = 1\,150\,000$ (■)

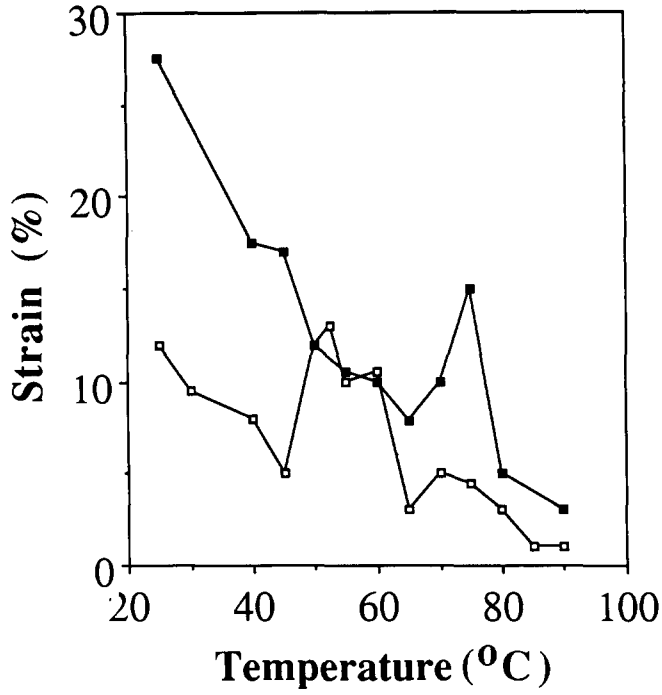

Figure 6 The median plastic strain for fibril breakdown ε_{pb} in PS as a function of temperature at a strain rate of $4 \times 10^{-6}\ m^{-2}$ for $M = 127\,000$ (□) and $M = 1\,150\,000$ (■)

(iii) For $M = 1\,150\,000$, ε_{pb} continues to decrease slightly with T above 40°C, but the dependence is not very marked up to approximately 65°C, at which temperature there is a sharp increase in ε_{pb}. As T approaches T_g, ε_{pb} drops away once more, although good statistics were hard to obtain in this regime. Again the minimum in ε_{pb} appears to correlate with the onset of a steep decrease in ε_c with T at approximately 65°C.

The morphology of breakdown also showed changes with T. At the lowest temperatures, the small characteristic pear-shaped cracks at the craze surfaces described by Kramer and coworkers[7,20] were observed for all M. However, as the maxima in ε_{pb} described above were traversed, the onset of breakdown appeared to be characterized by more extensive fibril failure, and at temperatures close to T_g involved catastrophic breakdown of the grid squares. It was also found, particularly for $M = 1\,150\,000$, that cracks tended to nucleate in the craze midrib close to T_g, and that the crazes were able to widen with little further apparent damage. The fact that close to T_g, only one or two crazes nucleated in each grid square, in contrast to the low-temperature behaviour, where the craze density became very high, suggested that the stress was not rising with ε_p close to T_g, and may have even have been falling. This would explain the apparent stability of wide crazes in this regime.

Results for poly(ether sulphone)

Some results for ε_c and ε_{pb} are given in *Figures 7* and *8* for the various molecular weights of PES. In this case the values of ε_{pb} do not represent an equivalent criterion to the one used for PS, since in most of the observations

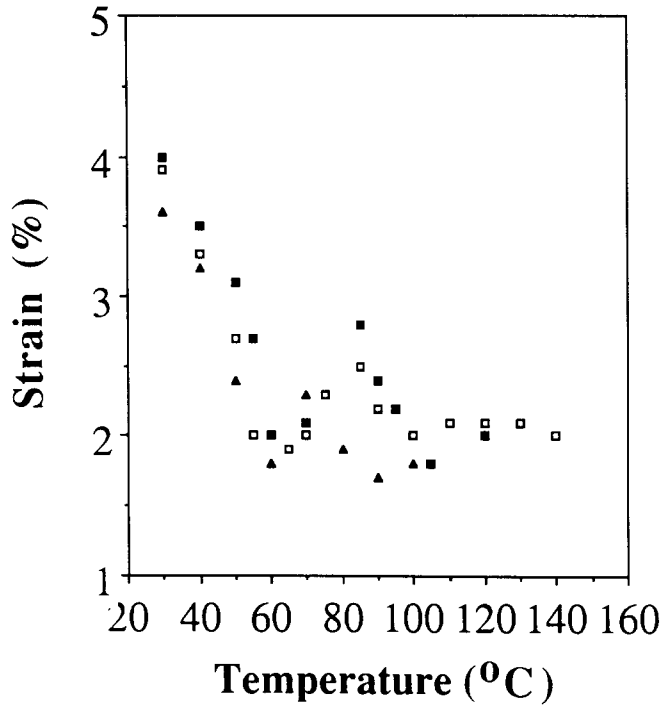

Figure 7 The strain to craze in PES as a function of temperature at a strain rate of 4×10^{-6} m^{-2} for M1 (□), M4 (■) and $M_w \sim 25\,000$ (▲)

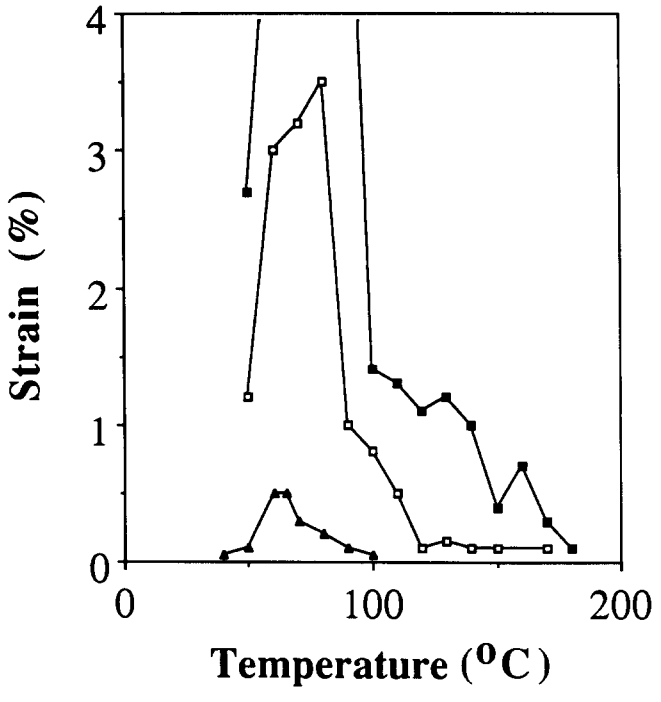

Figure 8 The median plastic strain for grid-square failure in PES as a function of temperature at a strain rate of 4×10^{-6} m^{-2} for M1 (□), M4 (■) and $M_w \sim 25\,000$ (▲)

of PES, the crazes did not grow to a sufficient width for it to be possible to observe small-scale perturbations within the craze body. Thus the first indication of fibril breakdown tended to be widespread fibril failure resulting in cracks several micrometres across. However, as suggested in ref. 20, there should be a correlation between the onset of breakdown and catastrophic failure, so that the model should remain qualitatively correct for data obtained in this way.

In *Figure 7*, there is a marked drop in the strain for deformation onset as T is increased, and this is associated with a transition from shear deformation to crazing in the sample as has been observed previously in PES[8]. The strain to craze ε_c appears to reach a minimum at approximately 60°C, and then rise slightly just above this temperature, before falling off again with T. This maximum was at a somewhat higher temperature for M1 and M4 than for the low-molecular-weight fraction. It had not been detected in previous observations[8] of ε_c in PES, carried out at a higher strain rate of approximately 10^{-2} s^{-1}. However, the presence of the peaks in the low-strain-rate results may be a consequence of the effect of multiple crossing on fibrillation; as argued elsewhere[19], because of the M^2 dependence of the mean force for disentanglement via the block-and-tackle mechanism, the onset of a small degree of chain scission may result in a decrease in the surface tension at the void tip as the temperature is lowered. (One scission event per chain, for example, would contribute little to Γ itself, but since it would decrease M by a factor of approximately 2, it will decrease the mean force for disentanglement by a factor of 4.)

The behaviour of ε_{pb} in PES is qualitatively similar to that of ε_{pb} in PS. For all three molecular weights in *Figure 8* there is an initial drop in ε_{pb} with increasing T, and then a maximum, coinciding with the maximum in ε_c, followed by decrease as T approaches T_g. At these higher temperatures and also at the low-T minimum in ε_{pb}, the crazes became very unstable, there being very little difference between ε_{pb} and ε_c, particularly for the low molecular weights. Such behaviour was also reflected by a marked decrease in the stability of the crazes formed in these regimes with respect to radiation damage when examined under TEM.

Unlike in PS, shear deformation, in the form of shear deformation zones (DZs)[2,3,8], was associated with high values of ε_p, even in regimes where the primary deformation was crazing. Also, in the low-molecular-weight samples, when crazes broke down at very low values of ε_p, the sudden local increase in strain rate and stress then appeared to favour shear deformation. As the DZs grew from the cracks and stabilized them, crazing was again favoured and subsequent crack nucleation gave rise to further shear deformation.

For the higher molecular weights of PES, DZs appeared as the strain was increased beyond ε_c. Once shear deformation has initiated, that is, once the upper yield stress has been reached, the flow stress for DZs is expected to be lower than that for crazing (this is implied by the complete suppression of crazing in PES that has not undergone a prior ageing treatment[8]). TEM confirmed that deformation zones had formed around pre-existing crazes, that is, as a continuation of the widening mechanism. Certainly at higher strains, because these DZs grew very wide, the crazes remained relatively small. Furthermore, when breakdown did occur, particularly in regimes where ε_{pb} was relatively large, it often did so in crazes lying along the centre line of DZs, suggesting that these crazes continue to grow slowly by fibrillation of the DZ material, even though the bulk of the extension is taken up by shear deformation.

This behaviour is consistent with earlier observations[13] in which the ductile–brittle transition with increasing temperature in macroscopic tensile test bars of PES was described. For the highest molecular weight, M4, and at

temperatures close to T_g, where thin-film results suggest that crazing should be favoured over shear deformation, it was found that crazes did not lead to catastrophic crack growth and embrittlement, but were stabilized instead by shear bands,which nucleated from the craze tips. The lower molecular weights on the other hand did show a transition to brittle behaviour, which can be rationalized in terms of both the decreased stability of the crazes and the fact that the crazing stress will be reduced relative to the yield stress.

Comparison of the results with theory

There is good qualitative agreement between the predicted behaviour of ε_{pb} for PS in *Figure 4* and the data of *Figure 6*. The temperatures at which the peaks in ε_{pb} occur correspond well in the two figures and, in particular, the model accounts well for the peak separation on the temperature axis for the two molecular weights. Comparison of the results for ε_c and the stability results for both PS and PES shows there to be a good correlation between the peaks in ε_{pb} and the onset of disentanglement associated with the sharp drop in ε_c with increasing T. Moreover, as may be seen from *Figures 7* and *8*, for PES the peaks in ε_{pb} also coincide well with the peaks in ε_c curves, which were identified with the possibility of a transition from a mixed scission/disentanglement regime to a disentanglement-only regime of crazing. This is again consistent with the model since it represents the point at which there is no longer degradation of the fibril molecular weight (in practice, however, the peak is expected to be smoothed out somewhat owing to the polydispersity of the PES samples).

Since the PS samples were monodisperse and, in particular, since shear deformation did not contribute to ε_p, one might expect quantitative agreement between the measured values of ε_{pb} and those in *Figure 4*. However the agreement is not good, which calls into question the details of the assumptions of the model. The basis of Kramer and Berger's justification of the Weibull approach[7] is the power-law form of equation (10). In this next part of the discussion, the validity of the assumption of power-law behaviour in equation (10) is examined, not only for the room-temperature behaviour of PS investigated by Kramer and Berger but also at higher T.

At room temperature, equation (10) may be derived by using a power-law approximation to the tail of the Gaussian cumulative density function, as has been done previously for similar weak-link problems[29]. This approach is valid when σ/μ for the distribution is less than approximately 0.5, where σ is the standard deviation and μ is the mean; for $q = 0.6$ (as in room-temperature crazing in PS[1]) equation (13) suggests that σ/μ is approximately 0.1, and it is found that, for a large range of probabilities (several decades) centred on $\phi(i)$ of the order of magnitude of 10^{-10}, the expression $\phi(i) \sim i^n$ is a good approximation, where n is approximately 20. In equation (11) $V_0 n_f$ is of the order of 10^{11}, which suggests that the observed ε_{pb} also reflect probabilities of the order of 10^{-11}.

It is also found from equation (16) that for $i < \frac{1}{2}n_0$, $\tau_{dis}(i) \sim BS^{-1}i$, where B is a front factor weakly dependent on M, but approximately independent of i, and S is given by equation (9). Since such i values correspond to values of $\phi(i)$ for which the power-law approximation is valid, we may use the following approach. It is assumed that breakdown occurs when $\tau_{dis}(i) < t_{res}$; this criterion is then used to define an i_c such that for all $i < i_c$ breakdown will take place and which is given by:

$$i_c \sim S_1 \varepsilon_p^w t_{res}/B \tag{20}$$

and since $\phi(i_c) \sim i_c^n$:

$$p_b(\varepsilon_p) \sim (S_1 \varepsilon_p^w t_{res}/B)^n = p_b(S_1)\varepsilon_p^{nw} \tag{21}$$

So that, in this limit, comparison of equations (21) and (10) gives:

$$\rho_w - 1 \sim nw \tag{22}$$

Since n is approximately 20, then the observed values of ρ_w of approximately 5 at room temperature in PS suggest a value of w of 0.2 or less, which is both reasonable and consistent with the assumptions of Kramer and others[7,20].

In general, however, n will be a rapidly increasing function of decreasing σ/μ (ref. 29), that is, n will increase as the amount of scission decreases. Hence, at the onset of disentanglement, as T increases, a rise in n is predicted. Although the approximations used above will begin to break down as this regime is entered, it is inferred from equation (22) that effective values of ρ_w will also increase in this regime, since the scatter in local fibril strengths will be decreasing. For the same reason, it is expected that breakdown will tend to become uniformly catastrophic rather than localized as T increased, which is consistent with the observations.

The work-hardening exponent w in equation (22) will be decreasing with T close to T_g. Indeed, as pointed out above, in contrast to the behaviour at lower T, very few crazes are found in each grid square close to T_g, even at high values of ε_p, which suggests little work hardening and that S remains approximately equal to S_1. On this basis, since $p_b(\varepsilon_p) \sim p_b(0)$, equation (21) implies that ρ_w should tend to 1 in this regime.

Figure 9 gives some values of ρ_w calculated from the data for PS $M = 127\,000$ using equation (11). A peak in ρ_w corresponding to the peak in ε_{pb} is seen, consistent with the above discussion. The value of ρ_w then falls off as T approaches T_g, which is consistent with a decreasing work-hardening rate. For $M = 1\,150\,000$ there is also some suggestion of a peak in ρ_w corresponding to the peak in ε_{pb}, although there is considerably more scatter in the data. Thus it is concluded that, although the predicted behaviour of ε_{pb} may not be quantitatively correct at elevated temperatures (and the use of adjusted values of ρ_w is not sufficient to improve the quantitative agreement between the model and the data), the observed behaviour of ρ_w is further evidence of the qualitative correctness of our ideas.

The effect of polydispersity

In view of the limitations already inherent in the model we do not attempt to treat intrinsic inhomogeneity in the fibrillar molecular weight arising from polydispersity quantitatively. However, it is expected that the additional sources of variation in the fibrillar molecular weight will tend to give rise to more weak spots than in a monodisperse material, and that weak spots will persist into regimes where there is no molecular-weight degradation arising from scission. Thus ε_{pb} is expected to be lower for a polydisperse material than for a monodisperse

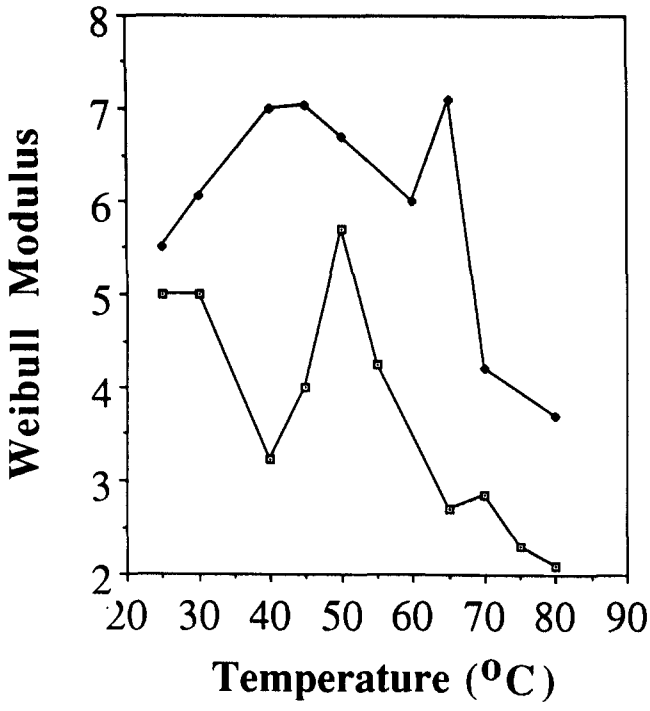

Figure 9 The temperature dependence of the Weibull modulus ρ_w in PS for $M = 127000$ (□) and $M = 1150000$ (■)

material of the same molecular-weight average. Preliminary data for PS $M = 127000$ and PS with a polydispersity of approximately 2 and a molecular-weight average of approximately 100000 suggest that the magnitude of ε_{pb} is severely depressed for the polydisperse material, and indeed catastrophic breakdown occurs at strains well below those at which the crazes have become wide enough for individual fibril breakdown events to be observed.

However, as suggested elsewhere[19], the presence of the low-molecular-weight tail may have a plasticizing effect (and here we take the term 'plasticization' to encompass such effects as tube renewal). Indeed, it is concluded from the fact that the molecular-weight distributions of the various grades of PES used in these investigations were very similar, that the changes observed in both the strain to craze and the strain for fibril breakdown are partly such a plasticization effect. This is also inferred from the relatively small shifts in the position on the T axis of the peaks in ε_c and ε_{pb} for the different molecular weights of PES, which in turn imply that the relative degrees of scission and disentanglement in the different samples remain approximately the same at any given temperature.

Similar plasticization effects may also be important for fibril breakdown by disentanglement in monodisperse materials in regimes where there is considerable chain scission during crazing, and consequently a broad fibrillar molecular-weight distribution. For the moment, however, the precise role that polydispersity plays in crazing and craze breakdown remains a matter for speculation.

CONCLUSIONS

We have modelled fibril breakdown as a function of temperature in terms of disentanglement of polymer chains in the 'active zone' at the craze–bulk interface, where the deformation ratio of the polymer is increasing towards that of the fully formed fibril, and the polymer is in a strain-softened state (that is, the chains are relatively mobile). This means that fibril stability will decrease markedly both with fibrillar molecular weight and also with T.

We have investigated craze fibril breakdown as a function of molecular weight and temperature in thin films of a variety of samples mounted on copper grids. As argued previously by Kramer and coworkers[7,20] the occurrence of one or more breakdown events in an individual grid square at a given plastic strain is assumed to be described in terms of the Weibull probability distribution, which may be directly related to variations in the fibril molecular weight. On the basis of the results it is argued that this approach accounts well for the qualitative behaviour of both PES and PS, both of which show peaks in fibrillar stability coinciding with a transition from scission-mediated crazing, with its associated fibrillar molecular-weight degradation, to disentanglement-mediated crazing, where there is no molecular-weight degradation. It is also found that for PES, and for relatively high molecular weights, fibril breakdown is prevented by the onset of shear deformation. This is consistent with earlier observations that crazing need not necessarily be associated with embrittlement in high-molecular-weight PES[16]. Finally it is noted from investigations of the effects of polydispersity that the onset of breakdown appears to be dominated by the extreme low-molecular-weight tail of the fibril molecular-weight distribution. This has important practical consequences for the toughness of nominally high-molecular-weight polymers whose molecular-weight distribution has an extensive low-molecular-weight tail. However, it is an effect for which a description may lie outside our simple ideas on disentanglement.

ACKNOWLEDGEMENTS

We gratefully acknowledge the support of ICI plc and useful discussions with Professor E. J. Kramer during the course of this work.

REFERENCES

1 Kramer, E. J. *Adv. Polym. Sci.* 1983, **52/53** (Ed. H. H. Kausch), Springer Verlag, Berlin, Ch. 1
2 Donald, A. M. and Kramer, E. J. *J. Polym. Sci., Polym. Phys. Edn.* 1982, **20**, 899
3 Donald, A. M. and Kramer, E. J. *J. Mater. Sci.* 1981, **16**, 2967
4 Donald, A. M. and Kramer, E. J. *Polymer* 1982, **23**, 461
5 Kramer, E. J. 'Environmental Cracking of Polymers' (Ed. E. H. Andrews), Applied Science, Barking, 1979, Ch. 3
6 Verheulpen-Heymans, N. *Polymer* 1980, **21**, 97
7 Kramer, E. J. and Berger, L. L. *Adv. Polym. Sci.* 1990, **91/92**, 1
8 Plummer, C. J. G. and Donald, A. M. *J. Polym. Sci., Polym. Phys. Edn.* 1989, **27**, 235
9 Wellinghof, S. T. and Baer, E. J. *J. Appl. Polym. Sci.* 1978, **22**, 2025
10 Donald, A. M. *J. Mater. Sci.* 1985, **20**, 263
11 Berger, L. L. and Kramer, E. J. *Macromolecules* 1987, **20**, 1980
12 Plummer, C. J. G. and Donald, A. M. *J. Mater. Sci.* 1989, **24**, 1399
13 Plummer, C. J. G. and Donald, A. M. *J. Appl. Polym. Sci.* 1990, **41**, 1197
14 DeGennes, P. G. *J. Chem. Phys.* 1971, **55**, 572
15 Doi, M. and Edwards, S. F. *J. Chem. Phys.* 1971, **55**, 1789, 1802
16 McLeish, T. C. B., Plummer, C. J. G. and Donald, A. M. *Polymer* 1989, **30**, 1651
17 Kou, C. C., Phoenix, S. L. and Kramer, E. J. *J. Mater. Sci. Lett.* 1985, **4**, 459
18 Kramer, E. J. *Polym. Eng. Sci.* 1984, **24**, 761

19 Plummer, C. J. G. and Donald, A. M. *Macromolecules* 1990, **23**, 3929
20 Yang, A. C.-M., Kramer, E. J., Kou, C. C. and Phoenix, S. L. *Macromolecules* 1986, **19**, 2010
21 Weibull, W. *J. Appl. Mech.* 1951, **18**, 293
22 Döll, W., Schinker, M. G. and Konczol, M. *Int. J. Fracture* 1979, **15**, 145
23 Fellers, J. F. and Kee, B. F. *J. Appl. Polym. Sci.* 1974, **18**, 2355
24 Berger, L. L., Buckley, D. J., Kramer, E. J., Brown, H. R. and Bubeck, R. A. *J. Polym. Sci., Polym. Phys. Edn.* 1987, **25**, 1679
25 Davies, M. and Moore, D. R. ICI plc Internal Report, 1987
26 Beahan, P., Bevis, M. and Hull, D. *J. Mater. Sci.* 1973, **8**, 162
27 Lauterwasser, B. D. and Kramer, E. J. *Phil. Mag.* 1979, **20**, 469
28 Donald, A. M. and Kramer, E. J. *J. Mater. Sci.* 1982, **17**, 1871
29 Plummer, C. J. G. and Evetts, J. E. *IEEE Trans. Mag.* 1987, **MAG-23**, 1179